



**HAL**  
open science

## Channel Model and Optimal Core Scrambling for Multi-Core Fiber Transmission System

Akram Abouseif, Ghaya Rekaya-Ben Othman, Yves Jaouën

► **To cite this version:**

Akram Abouseif, Ghaya Rekaya-Ben Othman, Yves Jaouën. Channel Model and Optimal Core Scrambling for Multi-Core Fiber Transmission System. Optics Communications, 2019, pp.55. hal-02269943

**HAL Id: hal-02269943**

**<https://imt.hal.science/hal-02269943>**

Submitted on 20 Dec 2021

**HAL** is a multi-disciplinary open access archive for the deposit and dissemination of scientific research documents, whether they are published or not. The documents may come from teaching and research institutions in France or abroad, or from public or private research centers.

L'archive ouverte pluridisciplinaire **HAL**, est destinée au dépôt et à la diffusion de documents scientifiques de niveau recherche, publiés ou non, émanant des établissements d'enseignement et de recherche français ou étrangers, des laboratoires publics ou privés.



Distributed under a Creative Commons Attribution - NonCommercial 4.0 International License

# Channel Model and Optimal Core Scrambling for Multi-Core Fiber Transmission System

Akram Abouseif, Ghaya Rekaya-Ben Othman and Yves Jaouën

*LTCI, Télécom ParisTech, Université Paris Saclay, France  
Email: akram.abouseif@telecom-paristech.fr*

---

## Abstract

Space division multiplexing (SDM) is a potential candidate to increase the capacity of the conventional single mode fiber based transmission systems. Several multi-core fiber (MCF) structures have been proposed, each one is impaired by different core dependent loss (CDL) resulting from the fiber structure, crosstalk, splicing in the optical fiber link and inline components. One of the solutions to mitigate the CDL is the core scrambling. In this paper, we introduce three deterministic core scrambling strategies for different MCFs. The strategies show their efficiency to reduce the CDL compared to the random scrambling. Moreover, in order to estimate the CDL level and predict the system performance for any MCF structure, we propose a theoretical channel model depends on the system configuration and the number of core scrambling installed in the transmission link. Lastly, the optimal deterministic core scrambler is obtained for further reduction of the scramblers number.

*Keywords:* Fiber optics communications, MIMO, space division multiplexing

---

## 1. Introduction

The exponential growth in the demand for network bandwidth results to find alternative solutions in order to replace the conventional optical fiber that reached the fundamental Shannon limit. The space is the remaining degree of freedom to increase the data carrying capacity of single mode optical fiber [1]. The space division multiplexing (SDM) is approached through: (i) multi-mode fiber (MMF), utilizes more than one linearly polarized (LP) modes in single core by enlarging the fiber core diameter, (ii) multi-core fiber (MCF), several cores coexist in the same cladding where each core carries single mode and (iii) multi-core multi-mode fiber (Dense-SDM), where each core in MCF carries more than one mode [2]. The orthogonal spatial channels in each path can carry independent data streams and being compatible with the system component such as: optical amplifier and wavelength selective switches (WSSs) [3]. In this paper, we focus on studying the MCF transmission systems since the MMF has intensively investigated previously in [4] [5] [6].

The multiplexing capability induces major challenge which is the crosstalk between the different cores. The coupling between the cores is inversely proportional to the core pitch. Thus, several MCF structures have been manufactured to address either high number of core multiplexing or low crosstalk level [7] [8] [9]. Moreover, the misalignment losses difference between the cores is considered as significant problem limits the system performance. These effects induce the core dependent loss (CDL) as a result of having different losses. The CDL is a non-unitary effect impairing the transmission system, similar to the polarization dependent loss (PDL) on the polarization multiplexing (PolMux) and mode dependent loss (MDL) on multi-mode fiber (MMF) [10] [11].

The performance of the CDL-impaired MCF system is optimized by applying the maximum-likelihood (ML) detection [6]. In our work, we use the sphere decoder (SD) as ML decoder solution to avoid huge complexity of exhaustive search ML detection [12]. In our previous work [13], the CDL mitigation in long haul optical links can be done by applying the core scrambling that averages the accumulated losses. However, the random core scrambling technique has been proposed in order to mitigate the CDL and enhance the system performance at the cost of installing large number of random scramblers. Therefore, we introduce deterministic core scrambling strategy for different MCF structures. We show that the deterministic scrambling outperforms the random scrambling by reducing the CDL level and the installed scramblers in the link. In addition, we obtain the optimal number of deterministic core scramblers to obtain the minimum CDL value that can be achieved in each structure with fewest number of scramblers.

The transmission system configuration and the MCF geometrical structure determine the CDL level. Thus, obtaining a theoretical channel model which is compatible with these variables is necessary to predict the system performance. In this paper, we propose MCF channel model considering both crosstalk and misalignment loss level. The theoretical MCF channel model is function of the transmission system configurations and MCF parameters such as: core reflective index, crosstalk, the number of the splices and the number of core scramblers. Based on the channel model, we prove that the CDL has a Gaussian distribution and estimate the mean value of the CDL. In industry, the theoretical channel model is an important tool in order to guide the MCF system manufacturing by setting all the parameters before beginning the production.

In the remainder, Section. 2 introduces the considered MCF

structures which will be evaluated in our work. Section. 3 derives the theoretical channel model of the MCF fiber taking into account the crosstalk and the misalignment level in the system. Section. 4 evaluates the deterministic core scrambling strategies. Then, we obtain as well the theoretical channel model for the system with scrambling. In addition, we provide the optimal number of the deterministic core scramblers. Finally, Section. 5 concludes the paper.

## 2. MCF structures

The MCF is manufactured by using either homogeneous or heterogeneous cores. The coupling between the homogeneous cores is highly affected by the core pitch and the bending radius thus increasing the number of cores is a challenge in this case. In the heterogeneous cores, the propagation constant mismatch between the cores reduces the coupling effect which allows high core multiplexing. Moreover, the trench assistance is an additional technique that provides power confinement in each core so decreasing the coupling factor. In this work, we are interested in the most commonly used structures according to the literature. As shown in Fig.1, the considered MCFs are: **(A)** 7-core Heterogeneous MCF (7-core Hetero-MCF) [14], **(B)** 7-core Heterogeneous MCF with Trench Assisted (7-core Hetero-TA-MCF) [14] [15], **(C)** 12-core Heterogeneous MCF (12-core Hetero-MCF) [16], **(D)** 12-core Heterogeneous MCF with Trench Assisted (12-core Hetero-TA-MCF) [16], **(E)** 19-core Heterogeneous MCF (19-core Hetero-MCF) [17], **(F)** 19-core Homogeneous MCF (19-core Homo-MCF) [18] and **(H)** 32-core Heterogeneous MCF (32-core Hetero-MCF) [19]. We can classify the structures depending on the core coupling where it is high in structures **A**, **C** and **F** and low in **B**, **D**, **E** and **H**. In the other side, the structures can be categorized according to the number of different type of cores in the fiber. In **A**, **B** and **E** the fibers contain three type of cores while **C**, **D** and **H** the fibers are constructed by selecting two type of cores. Lastly, structure **F** is the only fiber that contains homogeneous cores. Fig.2 illustrates the core index profile with and without trench assistance. The core radius, the distance between the core center and the inner edge of the trench and the distance between the core center are  $a_1$ ,  $a_2$  and  $a_3$ , respectively.  $W_{tr}$  is the trench thickness.  $n_0$  the refractive indices for the the 1<sup>st</sup> and 2<sup>nd</sup> cladding.  $\Delta_1$  is the relative refractive index differences between the core and 1<sup>st</sup> cladding and  $\Delta_2$  is the relative refractive index differences between trench and 2<sup>nd</sup> cladding. The cladding diameter in the {7, 12}-core MCF ( $CD_1$ ) is equal to  $125\mu_m$  while in the 19-core MCF the cladding diameter ( $CD_2$ ) is equal to  $210\mu_m$  and ( $CD_3$ ) is equal to  $243\mu_m$  in the 32-core MCF. Finally, the core parameters which have been considered for each layout are illustrated in Table.1.

## 3. Multi-Core Fiber Transmission System

### 3.1. System Model

The non-linearity related to Kerr effects is not considered supposing a limited transmission power which does not allow

reaching the non-linearity. Also, the deferential mode delay is not consider since it doesn't affect the capacity of the system and it can be perfectly mitigated by using Time Domain Equalizer or Frequency Domain Equalizer as it was done in [10]. In this section, we focus on the most challenging impairments that include core crosstalk, misalignment losses as well as the core dependent loss. We define and simulate a channel model of CDL-impaired transmission system.

#### 3.1.1. Crosstalk Channel Matrix

The coexist of the cores in the same cladding allows the energy to be transferred between the cores. The linear crosstalk between core  $n$  and core  $m$  ( $XT_{n,m}$ ) can be estimated based on the coupled-mode theory (CMT) or the coupled-power theory (CPT) [20]. However, the CPT has more accurate estimation by taking into account the fluctuation in the propagation constant. The crosstalk for homogeneous and heterogeneous cores are estimated by Eq.1 and Eq.2 [21], respectively.  $\beta$  and  $\Delta\beta$  are the propagation constant and the difference between the two cores.  $k_{nm}$  is the coupling coefficient.  $d$ ,  $L$  and  $\Lambda$  are respectively the correlation length, the fiber length and the core pitch. However, the coupling between the heterogeneous cores is gradually decreased when the bending radius  $R_b$  is greater than the radius of the crosstalk peak level  $R_{pk}$  ( $R_b > R_{pk}$ ), where  $R_{pk} = \frac{n_{eff}}{\Delta n_{eff}} \Lambda$  [15].  $n_{eff}$  and  $\Delta n_{eff}$  are the effective refractive index and the difference between two cores. In this case, Eq.2 is valid and the crosstalk becomes independent of the bending radius which gives the advantage of applying the heterogeneous MCF aiming to increase the number of cores.

$$XT_{n,m} = \frac{2k_{nm}^2 R_b}{\beta^2 \Lambda} L \quad (1) \quad XT_{n,m} = \frac{2k_{nm}^2}{\Delta\beta^2 d} L \quad (2)$$

For MCF with  $c$  number of cores, the crosstalk channel matrix  $\mathbf{H}_{XT}$  is given as:

$$\mathbf{H}_{XT} = \begin{bmatrix} XT_1 & XT_{1,2} & \cdots & XT_{1,c} \\ XT_{2,1} & \ddots & & XT_{2,c} \\ \vdots & & \ddots & \vdots \\ XT_{c,1} & XT_{c,2} & \cdots & XT_c \end{bmatrix}$$

where  $XT_i = 1 - \sum_{n \neq m} XT_{n,m}$ .

#### 3.1.2. Misalignment Losses Channel Matrix

Each core in the MCF is affected by different misalignment losses due to the imperfection at the splices, the connectors, the Fan-{In/out} devices and the fluctuation of the core positions [22] [23] [24]. There are three types of misalignment in single mode fiber: (i) longitudinal misalignment, (ii) transverse misalignment and (iii) angular misalignment [23]. In this work, we consider the transverse misalignment loss ( $\alpha$ ) since it has been proved that it has the main factor effecting the transmission system [25]:

$$\alpha = \exp(-br_d^2), \quad r_d = \sqrt{d_x^2 + d_y^2}, \quad b = \frac{2}{w_1^2 + w_2^2} \quad (3)$$

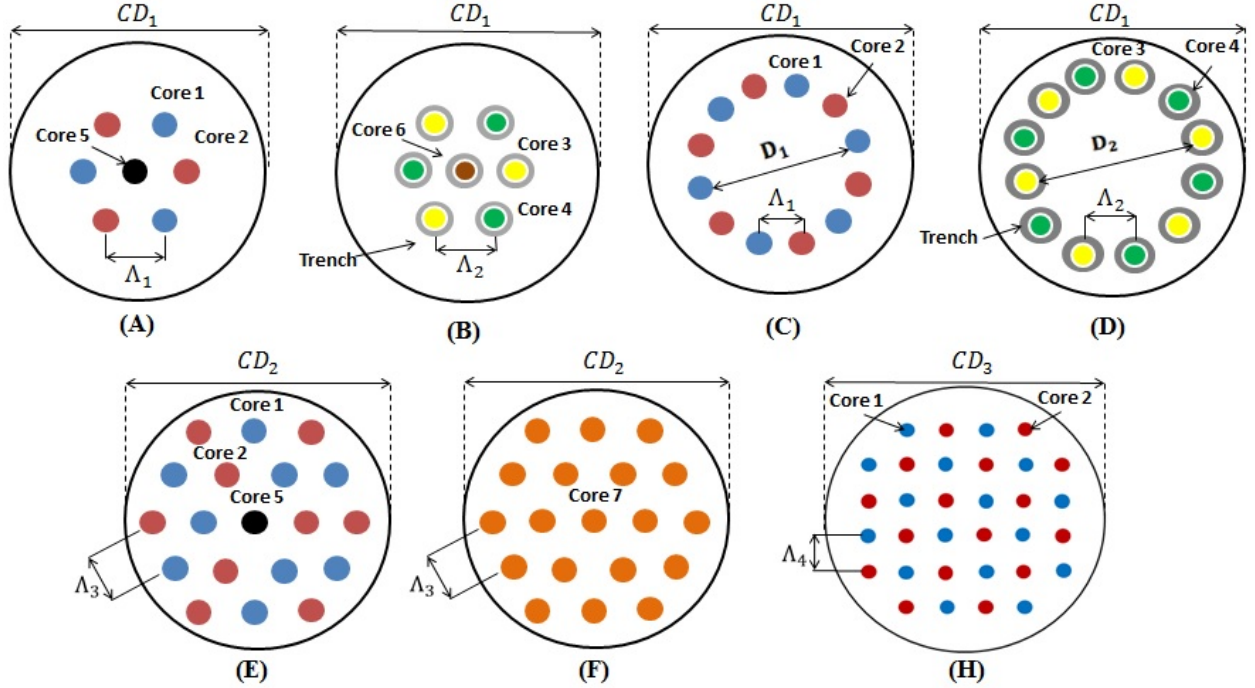


Figure 1: MCF structures, the cladding diameter  $CD_1 = 125\mu_m$ ,  $CD_2 = 210\mu_m$  and  $CD_3 = 243\mu_m$ , core pitch  $\Lambda_1 = 24\mu_m$ ,  $\Lambda_2 = 33\mu_m$ ,  $\Lambda_3 = 40\mu_m$  and  $\Lambda_4 = 33\mu_m$ ,  $D_1 < D_2$ .

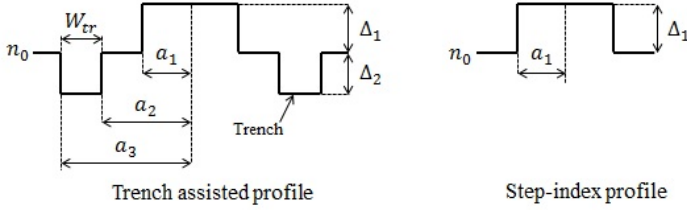


Figure 2: Core index profile

| core           | 1     | 2     | 3     | 4     | 5     | 6     | 7     |
|----------------|-------|-------|-------|-------|-------|-------|-------|
| $a_1[\mu_m]$   | 4.68  | 4.76  | 4.68  | 4.76  | 4.68  | 4.68  | 4.5   |
| $a_2/a_1$      | -     | -     | 1.7   | 1.7   | -     | 1.7   | -     |
| $W_{tr}/a_1$   | -     | -     | 1     | 1     | -     | 1     | -     |
| $n_0$          | 1.45  | 1.45  | 1.45  | 1.45  | 1.45  | 1.45  | 1.45  |
| $\Delta_1[\%]$ | 0.388 | 0.338 | 0.388 | 0.338 | 0.305 | 0.305 | 0.335 |
| $\Delta_2[\%]$ | -     | -     | 0.7   | 0.7   | -     | 0.7   | -     |

Table 1: Core parameters

$w_1$  and  $w_2$  are the fiber mode fields radius before and after the splicing, respectively.  $r_d$  is the transverse displacement of the fiber in the  $x$  and  $y$  directions.

The misalignment channel matrix  $\mathbf{M}$  for MCF single mode can be expressed as a diagonal matrix containing different loss values ( $diag(\alpha_1, \dots, \alpha_c)$ ). We assume the misalignment loss values as Gaussian random variables of zero mean and standard deviation ( $\sigma_{x,y}$ ) equal to  $\{ \%a_1 \}$  where  $a_1$  is the fiber core radius. Moreover, the cores endure different losses during the transmission and the gap increases by using heterogeneous cores spatially in long-haul transmission system.

### 3.1.3. Fiber model and Core Dependent Loss

Considering single mode with single polarization in each core for MCF structures, The resulting MIMO channel model is given by:

$$\mathbf{Y} = \mathbf{H}\mathbf{X} + \mathbf{N} = \sqrt{L} \prod_{k=1}^K ((\mathbf{H}_{XT})_k \mathbf{M}_k) \mathbf{X} + \mathbf{N} \quad (4)$$

where  $\mathbf{X}$  and  $\mathbf{Y}$  are respectively the emitted and the received vectors.  $\mathbf{H}$  is the channel matrix which is a concatenation of

$K$  fiber sections, each span is equivalent to the multiplication of the crosstalk channel matrix and the misalignment channel matrix.  $\mathbf{L} = \frac{c}{\sum_{i=1}^c \lambda_i}$  is a normalization factor used to compensate the link loss such that  $\text{Tr}(\mathbf{H}\mathbf{H}^H) = c$  (with  $\text{Tr}(\cdot)$  represent the trace of a matrix operator). Finally,  $\mathbf{N}$  is an Additive White Gaussian Noise with zero mean and variance  $N_0$ . In fact, the non-whiteness noise can be neglected in the case of the strong core coupling [18], However, in our model the white noise will be considered for all the coupling levels as it was done in [12] [26] [27] [28]. At the receiver side, the signals are detected by using the sphere decoder (SD). The CDL limits the transmission capacity of SDM system unlike the dispersive effects. In MIMO channel system, the CDL breaks the orthogonality of the parallel data streams which makes more difficult to retrieve the data at the receiver side. Therefore, keeping the CDL value as low as possible in the transmission link is important to obtain a channel close to the AWGN channel and reduce the decoding complexity at the receiver side. However, the CDL is defined as the ratio between the maximum eigenvalue ( $\lambda_{max}$ ) and the minimum eigenvalue ( $\lambda_{min}$ ) of  $\mathbf{H}\mathbf{H}^H$  in decibel where  $\mathbf{H}^H$  is the conjugate transpose of MCF channel model  $\mathbf{H}$

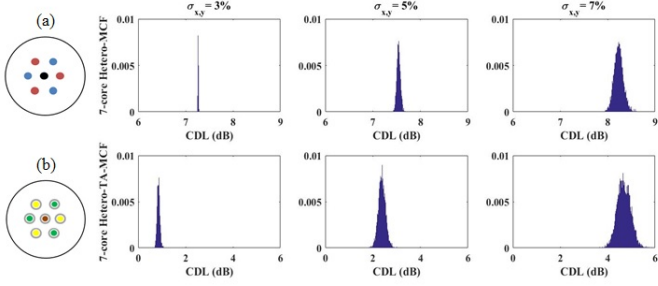


Figure 3: PDF of the CDL distribution for: (a) 7-core Hetero-MCF and (b) 7-core Hetero-TA-MCF with  $\sigma_{x,y} = \{3\%, 5\%, 7\% \} a_1$

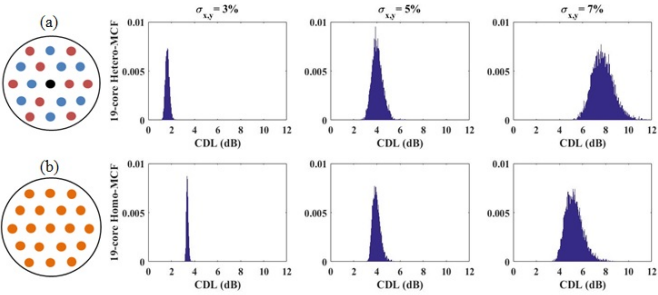


Figure 4: PDF of the CDL distribution for: (a) 19-core Hetero-MCF and (b) 19-core Homo-MCF with  $\sigma_{x,y} = \{3\%, 5\%, 7\% \} a_1$

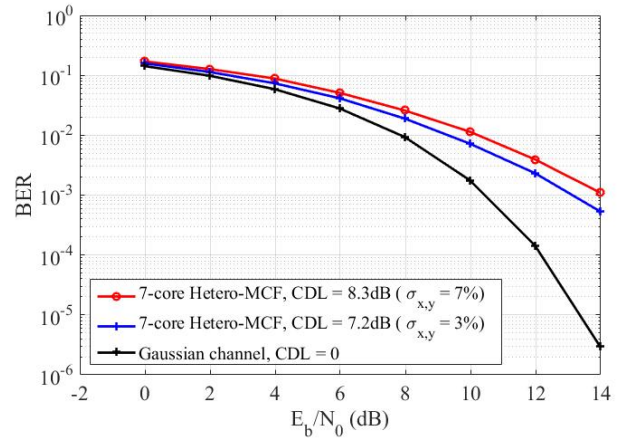
as:

$$CDL_{dB} = 10 \log_{10} \left( \frac{\lambda_{max}}{\lambda_{min}} \right) \quad (5)$$

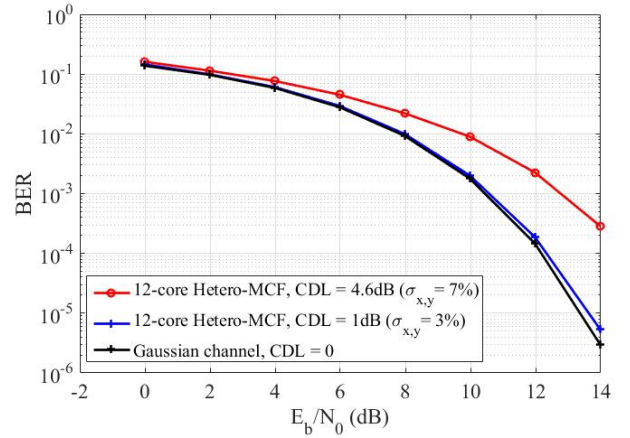
### 3.2. System Performance

In order to investigate the crosstalk and the misalignment effect on the CDL level, we simulate  $10^5$  channel realizations of several MCFs where  $K = 300$  misaligned fiber sections with  $\sigma_{x,y} = \{3\%, 5\%, 7\% \} a_1$ . Fig.[3,4], illustrate the PDF function of the CDL. In Fig.3, we compare between the 7-core Hetero-MCF and Hetero-TA-MCF where the crosstalk has been decreased by applying the trench assistance. We observe that the CDL level is directly proportional to the misalignment offset and the crosstalk level. Moreover, in Fig.4 we compare the 19-core Hetero-MCF and Homo-MCF. We notice that the homogeneous cores can be solution to reduce the CDL from  $8dB$  to  $5dB$  but at the cost of increasing the core pitch so enlarge the cladding diameter. The heterogeneous cores has increasing impact on the CDL since it forces the signals to follow different paths despite decreasing the core coupling spatially for long-haul transmission systems. Thus, applying heterogeneous or homogeneous cores doesn't necessary determine the CDL level caused by the losses induced in the system.

Further, we plot the bit error rate ( $BER$ ) versus the signal to noise ratio  $SNR = 10 \log_{10}(E_b/2N_0)$  for different CDL values corresponding to  $\sigma_{x,y} = \{3\%, 7\% \} a_1$ . A 16-QAM modulation is used at the transmitter and sphere decoder (SD) is used at the receiver side. In Fig.5(a), we show the performance of structure A. We observe SNR penalty equal to  $1.5dB$  at  $BER = 10^{-3}$  with  $CDL = 7.2dB$  compared to the Gaussian channel ( $CDL =$



(a) 7-core Hetero-MCF



(b) 12-core Hetero-MCF

Figure 5: BER performance: (a) 7-core Hetero-MCF and (b) 12-core Hetero-MCF, with  $3\% a_1$  misalignment level (red curve) and  $7\% a_1$  misalignment level (blue curve).

$0$ ) and  $2.5dB$  penalty with  $CDL = 8.3dB$ . Moreover, we evaluate the performance of configuration C as shown in Fig.5(b). We notice that the system performance with CDL value equal to  $1dB$  has SNR penalty =  $0.1dB$  at  $BER = 10^{-3}$  and the penalty increases to  $2dB$  with  $CDL = 4.6dB$ . Finally, we plot the average capacity as in [10] for the 7-core Hetero-MCF and 19-core Hetero-MCF versus the  $SNR$ . In Fig.6, we observe that the capacity of the system increases with the increasing number of cores. Also, we notice the effect of the misalignment which induces more CDL in the system so decrease the system capacity.

### 3.3. Theoretical Channel Model

In the previous section, we have shown the CDL impact on the MCF system performance. The transmission system configuration and the MCF structure determine the CDL level. Thus, deriving theoretical channel model as a tool to estimate the CDL for all MCF systems is required. In this section, we aim to model the MCF channel  $\mathbf{H}$  theoretically by using the singular value decomposition as:  $\mathbf{H} = \mathbf{U}\mathbf{\Sigma}\mathbf{V}^H$ , where  $\mathbf{U}$  and  $\mathbf{V}^H$  are random unitary matrices and  $\mathbf{\Sigma}$  is a diagonal matrix with singular

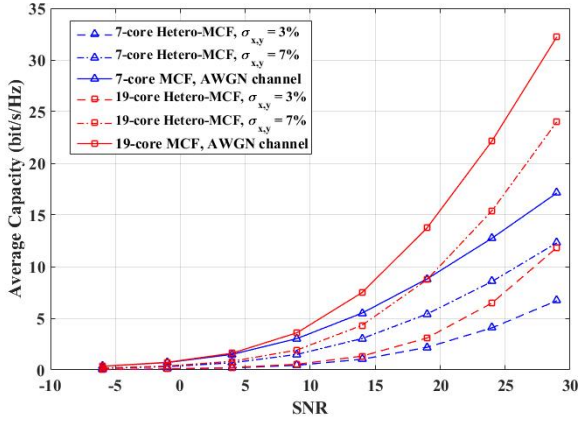


Figure 6: The average capacity versus the SNR for: the 7-core Hetero-MCF and 19-core Hetero-MCF with  $\sigma_{x,y} = \{3\%, 7\%\}a_1$  and  $K = 300$

value elements  $\lambda_i$ .

The equivalent channel matrix  $\mathbf{H}$  is a concatenation of each section as:

$$\mathbf{H} = \underbrace{(\mathbf{H}_{XT})_1 \mathbf{M}_1}_{\mathbf{H}_1} \underbrace{(\mathbf{H}_{XT})_2 \mathbf{M}_2}_{\mathbf{H}_2} \dots \underbrace{(\mathbf{H}_{XT})_K \mathbf{H}_K}_{\mathbf{H}_K} \quad (6)$$

By applying the QR decomposition (see Appendix Appendix A) starting from the last section ( $\mathbf{H}_K$ ). Then, we apply the QR decomposition on the previous section  $\mathbf{H}_{K-1}$  after multiplying by the orthogonal matrix  $\mathbf{Q}_K$ :

$$\begin{aligned} \mathbf{H} &= \mathbf{H}_1 \mathbf{H}_2 \dots \mathbf{H}_{K-1} \underbrace{\mathbf{H}_K}_{\mathbf{Q}_K \mathbf{R}_K} \\ &= \mathbf{H}_1 \mathbf{H}_2 \dots \underbrace{\mathbf{H}_{K-1} \mathbf{Q}_K}_{\mathbf{Q}_{K-1} \mathbf{R}_{K-1}} \mathbf{R}_K \end{aligned} \quad (7)$$

The multiplication of the unitary matrix  $\mathbf{Q}$  doesn't change the value of the upper triangular of each  $\mathbf{R}_k$ ,  $k \in [1, \dots, K]$ . Finally, we continue the process until reaching  $\mathbf{Q}_1$  which is the equivalent unitary matrix of the product:

$$\mathbf{H} = \mathbf{Q}_1 \mathbf{R}_1 \mathbf{R}_2 \dots \mathbf{R}_K \quad (8)$$

where the diagonal value of each  $\mathbf{R}_k$  approximately can be given as:

$$r_i = \alpha_i^k \sqrt{XT_i^2 + \sum_{j=1}^c XT_{i,j}^2} \quad (9)$$

The singular values of the equivalent channel  $\mathbf{H}$  are equal to the diagonal values of the product of  $\mathbf{R}_k$  given that  $\mathbf{Q}$  is a unitary matrix. Hence, the singular values are equal to:

$$\lambda_i = \prod_{k=1}^K r_i^k = \prod_{k=1}^K (\alpha_i^k \sqrt{XT_i^2 + \sum_{j=1}^c XT_{i,j}^2}) \quad (10)$$

Based on the singular values distribution behaviour, obtaining the CDL differs from heterogeneous MCF and homogeneous MCF. Thus, The following explains in details the CDL derivation for both cases.

### 3.3.1. Heterogeneous MCF

For simplification, the summation of the crosstalk squared ( $\sum_{j=1}^c XT_{i,j}^2$ ) can be neglected since it has been noticed that the values are very small compared to  $XT_i^2$ . Therefore, the singular values are expressed as:

$$\lambda_i = (XT_i)^K \prod_{k=1}^K \alpha_i^k \quad (11)$$

$(XT_i)^K$  and  $\alpha_{i,total} = \prod_{k=1}^K \alpha_i^k$  are respectively the total crosstalk and the total misalignment losses of core  $i$  at the end of the link where:

$$\alpha_{i,total} = \prod_{k=1}^K \alpha_i^k = \exp(Z), \quad Z = \sum_{k=1}^K -b(dx_{k,i}^2 + dy_{k,i}^2) \quad (12)$$

$dx_{k,i}^2$  and  $dy_{k,i}^2$  are Chi-squared distributed with 1 degree of freedom  $\sim \sigma_{x,y}^2 \tilde{\chi}_1^2$ . So,  $dx_{k,i}^2$  and  $dy_{k,i}^2$  have mean  $\sigma_{x,y}^2$  and variance  $2\sigma_{x,y}^4$ . For high number of sections  $K$ , we can apply the Central Limit Theorem (CLT) on  $Z$ . This leads to set that  $Z$  is normally distributed with mean  $\mu_z = -2Kb\sigma_{x,y}^2$  and variance  $\sigma_z^2 = 4Kb^2\sigma_{x,y}^4$ .

As  $Z$  is normally distributed,  $\alpha_{i,total} = \exp(Z)$  has a lognormal distribution with parameters:

$$\mu_{\alpha_{i,total}} = \exp(\mu_z + \sigma_z^2/2) = \exp(2Kb_i(b_i\sigma_{(x,y)_i}^4 - \sigma_{(x,y)_i}^2)) \quad (13)$$

$$\sigma_{\alpha_{i,total}}^2 = (\exp(\sigma_z^2) - 1) * \mu_{\alpha_i}^2 = (\exp(4Kb_i^2\sigma_{(x,y)_i}^4) - 1) * \mu_{\alpha_i}^2 \quad (14)$$

thus  $\lambda_i$  is lognormally distributed with mean  $(XT_i)^K \mu_{\alpha_{i,total}}$  and variance  $(XT_i)^{2K} \sigma_{\alpha_{i,total}}^2$ .

Obtaining the singular values distribution for each core allows to estimate the CDL value theoretically. Applying Eq.13 and Eq.14 to determine each of the maximum and the minimum eigenvalue ( $\lambda_{max}, \lambda_{min}$ ). Thus, the CDL has a Gaussian distribution  $\mathcal{N}(\mu_{CDL}, \sigma_{CDL})$  where:

$$\mu_{CDL} = \left(\frac{20}{\ln(10)}\right) \times \left(K \ln\left(\frac{XT_{max}}{XT_{min}}\right) + (\mu_{z,\lambda_{max}} - \mu_{z,\lambda_{min}})\right), \quad (15)$$

$$\sigma_{CDL} = \left(\frac{20}{\ln(10)}\right)^2 \times (\sigma_{z,\lambda_{max}}^2 + \sigma_{z,\lambda_{min}}^2) \quad (16)$$

### 3.3.2. Homogeneous MCF

In case of heterogeneous MCF, it's clear to define  $\lambda_{max}$  and  $\lambda_{min}$  by determining the singular values with maximum and minimum means ( $\mu_{max}, \mu_{min}$ ). In the other side, the homogeneous cores follow the same lognormal distribution which leads to obtain each of  $\mu_{max}$  and  $\mu_{min}$  by using different methodology.

The CDF of  $\max\{\lambda_i\}$  and  $\min\{\lambda_i\}$  are respectively defined as  $F(x)^n$  and  $1 - (1 - F(x))^n$  where  $F(x)$  is the CDF of random variable  $\lambda_i$ .

Since  $Z \sim \mathcal{N}(\mu_z, \sigma_z)$ , the PDF of  $X = \min\{Z\}$  and  $Y = \max\{Z\}$  are given as (see Appendix. Appendix B):

$$f_X(z) = \frac{n}{\sigma_z \sqrt{2\pi}} \left[ \operatorname{erfc}\left(\frac{z - \mu_z}{\sigma_z \sqrt{2\pi}}\right) \right]^{n-1} e^{-\left(\frac{z - \mu_z}{\sigma_z \sqrt{2\pi}}\right)^2} \quad (17)$$

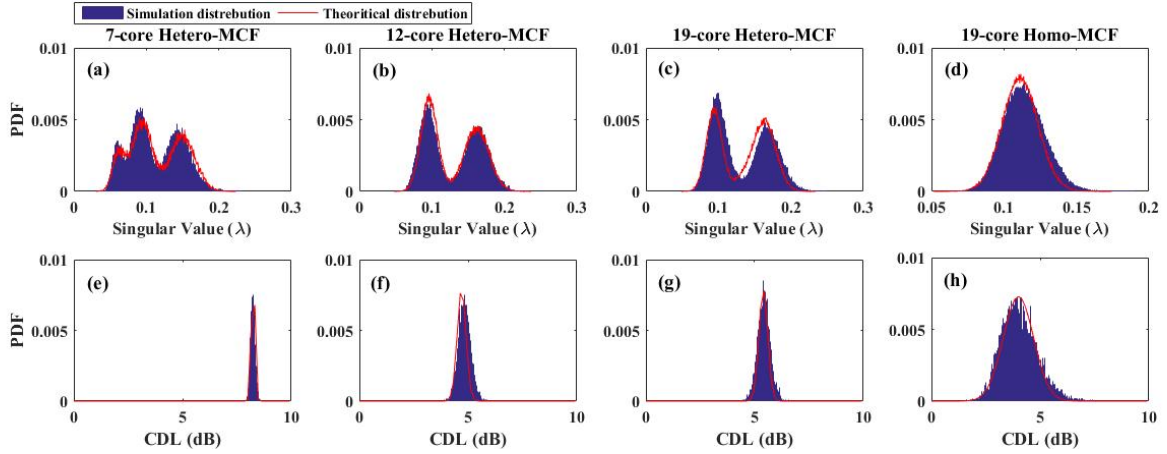


Figure 7: Comparison between the simulated and the Theoretical PDF distribution, the upper figures are the PDF of the singular value and the bottom figures are the PDF of the CDL

$$f_Y(z) = \frac{-n}{2^{n-2}\sigma_z\sqrt{2\pi}} \left[ 1 + \operatorname{erf}\left(\frac{z - \mu_z}{\sigma_z\sqrt{2\pi}}\right) \right]^{n-1} e^{-\left(\frac{z - \mu_z}{\sigma_z\sqrt{2\pi}}\right)^2} \quad (18)$$

We notice that  $\sigma_z$  has a very small value which allow us to assume that  $\operatorname{erf}(\cdot)$  and  $\operatorname{erfc}(\cdot)$  reach the saturation. Therefore, we can claim that the PDF of the  $X$  and  $Y$  are normally distributed.

Further, the mean values of  $X$  and  $Y$  are given by [29]:

$$\mu_{max} = E[X] = \mu_z + \sigma_z E_c \quad (19)$$

$$\mu_{min} = E[Y] = \mu_z - \sigma_z E_c \quad (20)$$

where  $E_c$  is defined as:

$$E_c = \int_{-\infty}^{\infty} z \frac{d}{dz} F_z(z) dz \quad (21)$$

It has been shown in [29] that  $E_c$  can be approximated by  $E_c \sim \sqrt{2 \log(c)}$  which depends on the number of cores  $c$  in the MCF. Thus, the CDL can be rewritten as:

$$\mu_{CDL} = \left( \frac{20}{\ln(10)} \right) \times \left( \ln\left(\frac{XT_{max}}{XT_{min}}\right) + (2E_n\sigma_z) \right), \quad (22)$$

$$\sigma_{CDL} = \left( \frac{20}{\ln(10)} \right)^2 \times (2\sigma_z^2) \quad (23)$$

### 3.4. Channel model Validation

We compare the proposed theoretical channel model with the simulated results for specific MCF structures that serve our purpose of illustrating all the observations. However, the following results can be obtained for any MCF structure. We simulate  $10^5$  realizations of the optical channel where  $K = 300$  misaligned fiber sections with  $\sigma_{x,y} = 7\%a_1$ ,  $R_b$  is equal to  $140mm$ , the correlation length is equal to  $100m$  as in [30] and  $100km$  fiber length. In Fig.7, we plot in the upper figures the PDF of the singular values ( $\lambda$ ) of  $\mathbf{H}$ . In Fig.7(a,c), we observe three distributions which corresponds to the three kind of cores co-existing in the same structure, the third distribution in Fig.7(c) is overlapped in the middle of the two distributions with low

probability. The same observation in Fig.7(b) since we notice two distributions related to the two type of cores in structure C. The singular values in  $\mathbf{F}$  (homogeneous cores) follow one distribution as shown in Fig.7(d). Then, the bottom figures compare between the simulated and theoretical CDL by plotting the PDF of the CDL. We notice that the two distributions are in a good agreement for all the structures. However, in order to have statistical information about the fitting between the two probability distributions, we apply the Kullback–Leibler divergence that measures the difference between two distributions. For continuous random variables of two probability distributions  $P$  and  $Q$ , the Kullback is defined as [31]:

$$D_{KL}(P||Q) = \int_{-\infty}^{\infty} p(x) \log \frac{p(x)}{q(x)} dx \quad (24)$$

The divergence of 0 indicates that the two distributions exactly fit each other while the divergence of 1 indicates completely different behavior. We calculate the Kullback divergence for each MCF structure obtained in Fig.7, for the singular value distributions the Kullback divergence is around 0.1 while for the CDL distribution the divergence is around 0.01 that gives a complete validation of the accuracy of the theoretical channel model.

## 4. Multi-Core Fiber Transmission System with Core Scrambling

### 4.1. System Model with Scrambling

In our previous work [13], the core scrambling has been investigated to mitigate the CDL induced by the transmission system. In this section, we propose deterministic core scrambling strategies to obtain an optimal CDL degradation in the MCF transmission system. As shown in Fig.8, the transmission including the scrambling matrices is given by:

$$\mathbf{Y} = \mathbf{H}\mathbf{X} + \mathbf{N} = \sqrt{L} \prod_{k=1}^K ((\mathbf{H}_{XT})_k \mathbf{M}_k \mathbf{P}_k) \mathbf{X} + \mathbf{N} \quad (25)$$

where  $\mathbf{P}_k$  are the permutation matrices which represents the scramblers when  $k$  is equal to the scrambling period  $K_{scr}$  and identity matrices in other cases,  $k$  is multiple of the scrambling period  $K_{scr}$ .

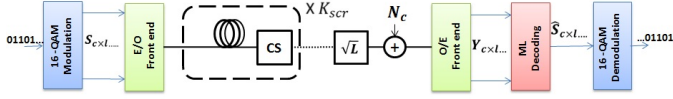


Figure 8: Multi-Core Fiber transmission system with random core scramblers

#### 4.2. Random and Deterministic Core Scrambling

The function of the core scrambling is illustrated in Fig.9. Assuming MCF with three different cores (black, red and blue), we send three messages in each core ( $S_1$ ,  $S_2$  and  $S_3$ ). Then, the scrambler is installed after  $K_{scr}$  and the signals are permuted randomly (random core scrambling) and transmitted through different core. In this case, the signals face the average losses induced by all the cores. However, installing large number of random core scramblers in the transmission link is the main drawback to approach a sufficient CDL reduction. Therefore, we propose a deterministic scrambling strategy, the aim is to make sure that in each scrambling period ( $K_{scr}$ ) the permutation of certain core should be with different core type. Thus, we propose three strategies for different MCF structures: (a) Snail scrambler, (b) Circular scrambler and (c) Snake scrambler shown in Fig.10. Switching from random core scrambling to deterministic scrambling makes the permutations matrices fixed after each  $K_{scr}$  in (25).

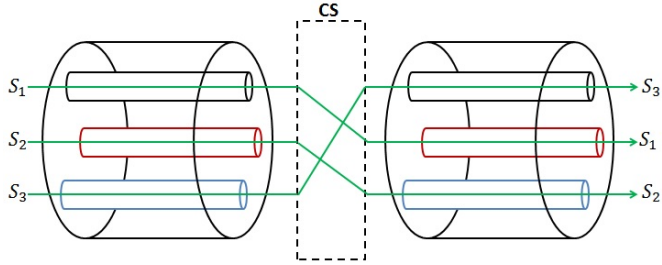


Figure 9: Core scrambling concept

A comparison between the random and deterministic scrambling is presented in Fig.11. We plot the CDL function of the number of the scramblers installed in the link where the number of sections  $K = 300$ . In Fig. 11(a), we notice that the CDL can be decreased to  $2.5dB$  in structure **A** (7-core Hetero-MCF) by installing only 5 deterministic scramblers instead of 35 random scramblers. Fig.11(b) illustrates the performance of the Circular scramblers in the ring structure **C** (12-core Hetero-MCF). We notice that in order to decrease the CDL level almost to the minimum which is equal to  $0.4dB$ , we need to install only 5 deterministic scramblers. Moreover, in structure **H** (32-core Hetero-MCF), we can decrease the number of scramblers from 35 random scramblers to 5 deterministic scramblers to obtain CDL equal to  $1.8dB$  as shown in Fig.11(c).

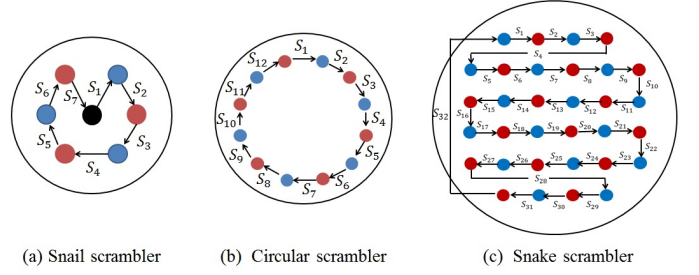


Figure 10: Deterministic scramblers strategies: (a) Snail scrambler, (b) Circular scrambler and (c) Snake scrambler

Further, we evaluate the performance of the three deterministic scrambling strategies. In Fig.12, we plot the bit error rate ( $BER$ ) versus the signal to noise ratio  $SNR = E_b/2N_0$  with the same configuration in Sec. 3. Starting with the Snail scramblers for the structure **A** in Fig.12(a), we notice that the 7-core Hetero-MCF without scrambling has  $SNR$  penalty equal to  $2dB$  at  $BER = 10^{-3}$  compared to Gaussian channel. Installing 5 Snail scramblers in the transmission link decreases  $SNR$  penalty to  $0.5dB$  instead of  $1dB$  by applying the random scramblers at  $BER = 10^{-3}$ . In Fig.12(b), we observe that installing 5 Circular scramblers for structure **C** mitigates completely the CDL from  $2.5dB$   $SNR$  penalty without scrambling and  $1.5dB$  penalty with random scrambling. Finally, Fig.12(c) illustrates the performance of the Snake scramblers for structure **H**, the system without scrambling has  $SNR$  penalty equal to  $2.5dB$  at  $BER = 10^{-4}$ . However, installing the random scramblers decreases the penalty to  $0.4dB$  while applying the Snake scramblers strategy reducing the  $SNR$  penalty to  $0.1dB$  by utilizing only 5 scramblers. However, the optimal number of deterministic scramblers to be installed in the system has to be determined. Therefore, obtaining the theoretical channel model with core scrambling is necessary to answer this question.

#### 4.3. Theoretical Channel Model with Scrambling

With the same methodology in section.3.3, we propose a theoretical channel model for MCF transmission system with deterministic core scrambling as  $\mathbf{H} = \mathbf{U}\Sigma\mathbf{V}^H$ . The theoretical model will lead to obtain the optimal number of deterministic scramblers.

##### 4.3.1. Derivation

The equivalent channel matrix  $\mathbf{H}$  in (25) with core scrambling is given as:

$$\mathbf{H} = \prod_{k=1}^K ((\mathbf{H}_{XT})_k \mathbf{M}_k \mathbf{P}_k) \quad (26)$$

By permuting the misalignment channel matrix  $\mathbf{M}_k$ , we obtain:

$$\mathbf{H} = \prod_{k=1}^K ((\mathbf{H}_{XT})_k \mathbf{M}_{p,k}) \quad (27)$$

where  $\mathbf{M}_{p,k}$  is the matrix after the permutation. Then, we apply the  $\mathbf{QR}$  decomposition with the same steps in section. 3.3. The

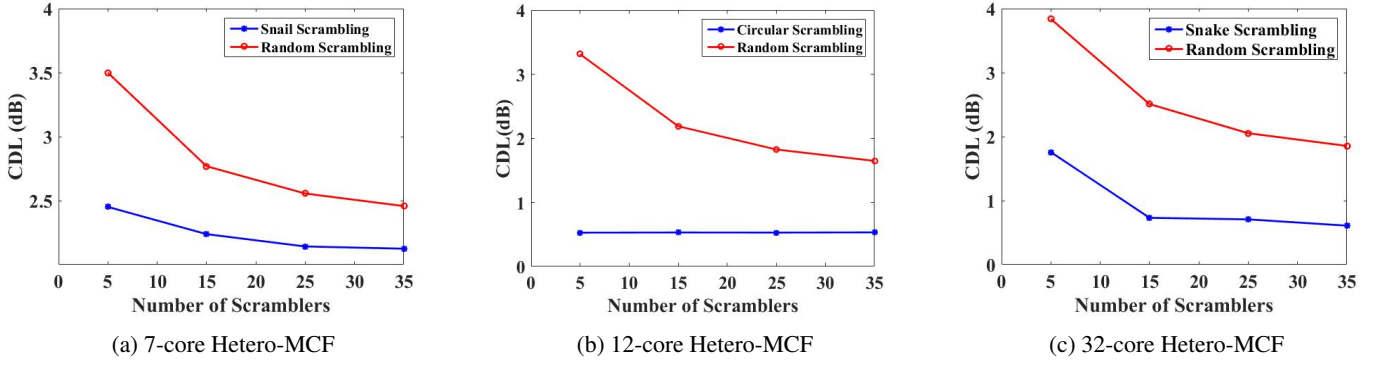


Figure 11: Comparison between the deterministic scramblers and random scramblers with number of section equal to 300

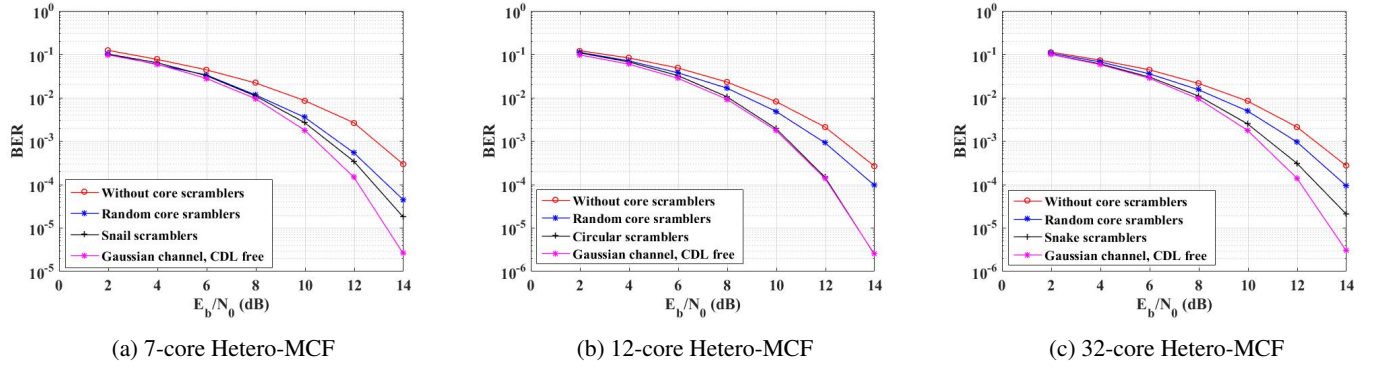


Figure 12: System performance without scrambling, with random scrambling and with deterministic scrambling after applying 5 core scramblers.

channel matrix  $\mathbf{H}$  can be expressed as:

$$\mathbf{H} = \underbrace{(\mathbf{H}_{XT})_1 \mathbf{M}_{p,1}}_{\mathbf{H}_{p,1}} \underbrace{(\mathbf{H}_{XT})_2 \mathbf{M}_{p,2}}_{\mathbf{H}_{p,2}} \dots \underbrace{(\mathbf{H}_{XT})_K \mathbf{M}_{p,K}}_{\mathbf{H}_{p,K}} \quad (28)$$

$$= \mathbf{Q}_{p,1} \mathbf{R}_{p,1} \mathbf{R}_{p,2} \dots \mathbf{R}_{p,K} = \mathbf{Q}_{p,1} \mathbf{R}_{p,eq}$$

The product of  $\mathbf{R}_{p,k}$  matrices is a random combination of all the misalignment loss values  $\alpha$  existing in the system as a resulting of the permutation matrices. So, the diagonal value of the upper triangular  $\mathbf{R}_{p,eq}$  is given as:

$$r_{p,i} = \left( \prod_{k=1}^{K_1} \alpha_1^k \times \dots \times \prod_{k=1}^{K_T} \alpha_T^k \right) \left( \sqrt{XT_i^2 + \sum_{j=1}^c XT_{i,j}^2} \right)^K \quad (29)$$

By neglecting  $(\sum_{j=1}^c XT_{i,j}^2)$ , the singular values with scrambling ( $\lambda_{p,i}$ ) are equivalent to the diagonal value of the upper triangular matrix  $\mathbf{R}_{p,eq}$ :

$$\lambda_{p,i} = \underbrace{\left( \prod_{k=1}^{K_1} \alpha_1^k \times \dots \times \prod_{k=1}^{K_T} \alpha_T^k \right)}_{(\alpha_{p,i})_{total}} (XT_i)^K, \quad \text{where } i \neq j \quad (30)$$

$(\alpha_{p,i})_{total}$  is the total losses after the scrambling at the end of the link and it is given as:

$$(\alpha_{p,i})_{total} = \prod_{k=1}^{K_1} \alpha_1^k \times \dots \times \prod_{k=1}^{K_T} \alpha_T^k = \exp(Z_p), \quad (31)$$

$$Z_p = \underbrace{[-b_1 \sum_{k=1}^{K_1} (dx_{k,i}^2 + dy_{k,i}^2)]}_{X_1} \underbrace{-b_2 \sum_{k=1}^{K_2} (dx_{k,i}^2 + dy_{k,i}^2)}_{X_2} \dots \underbrace{-b_T \sum_{k=1}^{K_T} (dx_{k,i}^2 + dy_{k,i}^2)}_{X_T} \quad (32)$$

where  $T$  is the number of different type of cores.  $K_t$  are the number of sections correspond to each type of core where  $t \in [1, \dots, T]$ . After applying the Central Limit Theorem on each term.  $X_t$  is a normal distribution with mean  $\mu_{X_t} = -2K_t b_t \sigma_{(x,y)_t}^2$  and variance  $\sigma_{X_t}^2 = 4K_t b_t^2 \sigma_{(x,y)_t}^4$ , which makes  $Z_p$  normally distributed with mean  $\mu_z = \sum_{t=1}^T \mu_{X_t}$  and variance  $\sigma_z^2 = \sum_{t=1}^T \sigma_{X_t}^2$ . Thus,  $(\alpha_{p,i})_{total} = \exp(Z_p)$  has a lognormal distribution with parameters:

$$\mu_{(\alpha_{p,i})_{total}} = \exp(\mu_z + \sigma_z^2/2) \quad (33)$$

$$\sigma_{(\alpha_{p,i})_{total}}^2 = (\exp(\sigma_z^2) - 1) * \mu_{(\alpha_{p,i})_{total}}^2 \quad (34)$$

Finally,  $\lambda_{p,i}$  is lognormally distributed with mean  $(XT_i)^K \mu_{(\alpha_{p,i})_{total}}$  and variance  $(XT_i)^{2K} \sigma_{(\alpha_{p,i})_{total}}^2$ .

#### 4.3.2. Optimal number of scramblers

Obtaining the optimal number of deterministic scramblers ( $S_{opt}$ ) is achievable by using the proposed channel model in the previous section. However,  $S_{opt}$  occurs when all the cores almost have the same losses during the transmission so obtaining

the minimum CDL value. The calculation of  $S_{opt}$  differ from one structure to another. In general,  $S_{opt}$  is the number of steps in order to reach all the cores  $S_{opt} = c - 1$ , where  $c$  is the number of cores. In the ring structures (**C** and **D**) is considered as special case where  $S_{opt} = T/2$ , where  $T$  is the number of different type of cores. In Fig.13, we plot the CDL function of the number of core scramblers. We observe that  $S_{opt} = 1$  for structure **C** since it has two type of cores ( $T=2$ ). On the other side, structures **A** and **H** respectively have  $S_{opt} = 6$  and 31 which proved our formulas.

Achieving the optimal deterministic scrambling allows to obtain the  $K_t$  values in Eq.32 since the permutations are known in this case:

$$K_t = K \times w_t, \quad (35)$$

where  $w_t = \frac{N_t}{c}$ ,  $N_t$  is the number of cores with the same type and  $c$  is the total number of cores.

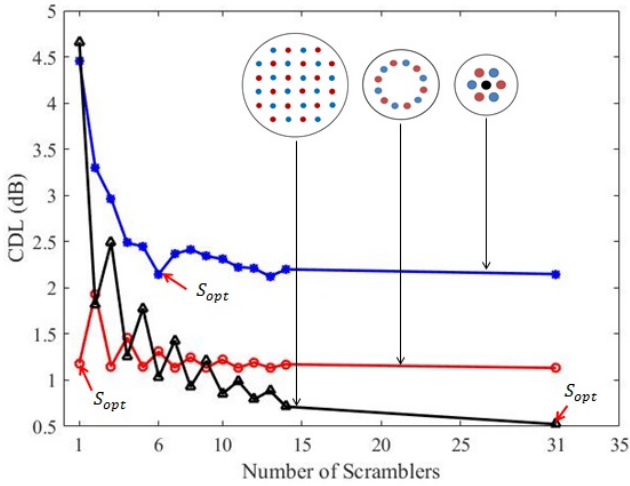


Figure 13: The CDL function of the number of deterministic scramblers

#### 4.4. Channel Model with Scrambling Validation

With the same simulation settings in section.3, we validate the theoretical channel model with deterministic core scrambling. We apply Eq.35 for the two ring structures (**C** and **D**) which leads to set both  $K_1$  and  $K_2$  to 150. In the case of structures **A** and **B**, we set the values of  $K_1$ ,  $K_2$  to be equal to 150 and  $K_3$  to 50. In Fig.14, we plot the PDF function of the singular value decomposition after the scrambling. First, we notice the effect of the scrambling since all the cores follow single distribution. Second, we observe that the theoretical results fit the simulation with Kullback divergence around 0.01.

## 5. Conclusion

In this paper, we have shown the CDL effect on the MCF transmission system. The aim of the paper is to introduce a theoretical model which allows to estimate the PDF distribution of the CDL in the system for several structures (homogeneous and heterogeneous) MCFs without and with core scrambling.

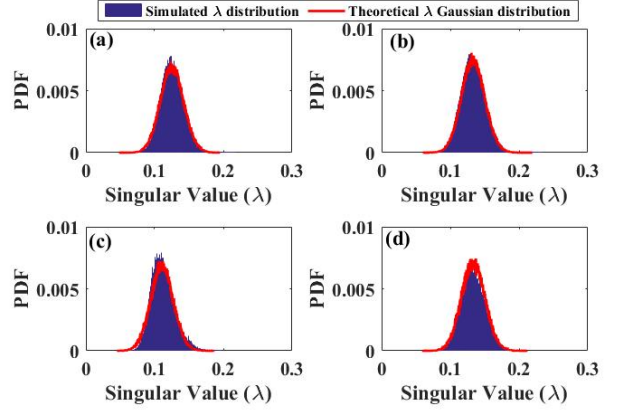


Figure 14: Simulated and Theoretical PDF of the singular value ( $\lambda$ ) with Optimal deterministic scrambling for: (a) 12-core Hetero-MCF, (b) 12-core Hetero-TA-MCF, (c) 7-core Hetero-MCF and (d) 19-core Homo-MCF

The theoretical model is a promising solution in order to predict the transmission system performance given some of the fiber parameters and the system configuration. Further, we proposed three deterministic scrambling strategies: Snake scrambling, Circular scrambling and Snake scrambling. These scramblers have the ability to obtain a sufficient CDL reduction by installing few number of scramblers compared to the random method. The optimal number of the deterministic scrambling was investigated over the three scrambling strategies. In the future, We are looking forward to lead experimental studies to validate the proposed theoretical channel model through experimental setup. Moreover, we aim to investigate the performance of the space time coding (STC) in MCF as alternative or complementary solution to the core scrambling.

## Appendix A. QR Decomposition

The QR decomposition also called QR factorization of a real square  $N \times N$  matrix  $\mathbf{H}$  is a decomposition of  $\mathbf{H}$  into an orthogonal matrix  $\mathbf{Q}$  and an upper triangular matrix  $\mathbf{R}$  such as:

$$\mathbf{H} = \mathbf{Q}\mathbf{R} \quad (A.1)$$

If  $\mathbf{H}$  is non-singular, the factorization is unique. There are several methods for computing the QR decomposition, the popular one is the Gram-Schmidt process. Consider the columns  $h_i, \{i: 1 \rightarrow N\}$  of  $\mathbf{H}$ . The Gram-Schmidt orthonormalization consists of:

$$u_1 = h_1, e_1 = \frac{u_1}{\|u_1\|}, \quad (A.2)$$

$$u_2 = a_2 - \langle a_1, e_1 \rangle e_1, e_2 = \frac{u_2}{\|u_2\|}, \quad (A.3)$$

$$u_{k+1} = a_{k+1} - \langle a_{k-1}, e_1 \rangle e_1 - \dots - \langle a_{k-1}, e_k \rangle e_k, \quad (A.4)$$

$$e_{k+1} = \frac{u_{k+1}}{\|u_{k+1}\|},$$

where  $\|\cdot\|$  is the Euclidean norm and  $\langle a, b \rangle = a^T b$  is the scalar product of two column vectors. The resulting QR factorization yields:

$$\mathbf{H} = \mathbf{QR} = \mathbf{Q} \begin{bmatrix} \langle a_{k-1}, e_1 \rangle & \langle a_{k-1}, e_N \rangle & \cdots & \langle a_2, e_N \rangle \\ 0 & \langle a_{k-1}, e_1 \rangle & & \vdots \\ \vdots & & \ddots & \\ 0 & \cdots & \cdots & \langle a_{k-1}, e_1 \rangle \end{bmatrix}$$

## Appendix B. The PDF of the maximum and minimum of normal distribution

We drive the PDF of  $U = \max\{X\}$  and  $V = \min\{X\}$  where  $X$  is normal distribution with mean  $\mu$  and standard deviation  $\sigma$ .

The normal distribution has CDF as:

$$F(x) = \frac{1}{2} \left[ 1 + \operatorname{erf} \left( \frac{x - \mu}{\sigma \sqrt{2}} \right) \right] \quad (\text{B.1})$$

Assuming  $G_U(x)$  is the CDF of  $U$  which is equal to  $(F(x))^n$ , where  $n$  is the number of sample of independent and identically distributed random variables. Also,  $G_V(x)$  is the CDF of  $V$  which is equal to  $1 - (1 - F(x))^n$ .

The PDF is obtained by taking the derivative of the CDF. In this case, the PDF of  $G_U(x) = n F(x)^{n-1} f(x)$ , which is given as:

$$f_U(x) = \frac{-n}{2^{n-2} \sigma \sqrt{2\pi}} \left[ 1 + \operatorname{erf} \left( \frac{x - \mu}{\sigma \sqrt{2}} \right) \right]^{n-1} e^{-\left( \frac{x - \mu}{\sigma \sqrt{2}} \right)^2} \quad (\text{B.2})$$

And the PDF of  $G_V(x) = n(1 - F(x))^{n-1} f(x)$ , knowing that  $\operatorname{erfc}(x) = 1 - \operatorname{erf}(x)$ :

$$f_V(x) = \frac{n}{\sigma \sqrt{2\pi}} \left[ \operatorname{erfc} \left( \frac{x - \mu}{\sigma \sqrt{2}} \right) \right]^{n-1} e^{-\left( \frac{x - \mu}{\sigma \sqrt{2}} \right)^2} \quad (\text{B.3})$$

## References

- [1] T. Mizuno, H. Takara, K. Shibahara, A. Sano, Y. Miyamoto, Dense space division multiplexed transmission over multicore and multimode fiber for long-haul transport systems, *Journal of Lightwave Technology* 34 (2016) 1484–1493.
- [2] D. Richardson, J. Fini, L. Nelson, Space division multiplexing in optical fibres, *Nature Photonics* 7 (2013) 354–362.
- [3] K. Saitoh, S. Matsuo, Multicore fiber technology, *Journal of Lightwave Technology* 34 (2016) 55–66.
- [4] A. El Mehdi, Y. Jaouen, G. Rekaya-Ben Othman, Optimal mode scrambling for mode-multiplexed optical fiber transmission systems, in: *Signal Processing in Photonic Communications*, Optical Society of America, 2016.
- [5] E. Awwad, G. Rekaya Ben-Othman, Y. Jaouën, Space-time coding and optimal scrambling for mode multiplexed optical fiber systems, in: *IEEE International Conference in Communications*, 2015, pp. 5228–5234.
- [6] A. Lobato, F. Ferreira, B. Inan, S. Adhikari, M. Kuschnerov, A. Napoli, B. Spinnler, B. Lankl, Maximum-likelihood detection in few-mode fiber transmission with mode-dependent loss, *IEEE Photon. Technol. Lett.* 25 (2013) 1095–1098.
- [7] X. Xie, J. Tu, X. Zhou, K. Long, K. Saitoh, Design and optimization of 32-core rod/trench assisted square-lattice structured single-mode multicore fiber, *Opt. Express* 25 (2017) 5119–5132.
- [8] K. Takenaga, Y. Arakawa, S. Tanigawa, N. Guan, S. Matsuo, K. Saitoh, M. Koshiba, Reduction of crosstalk by trench-assisted multi-core fiber, in: *Optical Fiber Communication Conference/National Fiber Optic Engineers Conference*, Optical Society of America, 2011, p. OWJ4.
- [9] J. Tu, K. Saitoh, M. Koshiba, K. Takenaga, S. Matsuo, Design and analysis of large-effective-area heterogeneous trench-assisted multi-core fiber, *Optics express* 20 (2012) 15157–15170.
- [10] P. J. Winzer, G. J. Foschini, MIMO capacities and outage probabilities in spatially multiplexed optical transport systems, *Optics Express* 19 (2011) 16680–16696.
- [11] S. Warm, K. Petermann, Splice loss requirements in multi-mode fiber mode-division-multiplex transmission links, *Optics express* 21 (2013) 519–532.
- [12] E. Viterbo, J. Boutros, A universal lattice code decoder for fading channels, *IEEE Transactions on Information theory* 45 (1999) 1639–1642.
- [13] A. Abouseif, G. Rekaya-Ben Othman, Y. Jaouen, Core mode scramblers for ML-detection based multi-core fibers transmission, in: *Asia Communications and Photonics Conference*, Optical Society of America, 2017, pp. M1B–5.
- [14] Y. Sasaki, Y. Amma, K. Takenaga, S. Matsuo, K. Saitoh, M. Koshiba, Investigation of crosstalk dependencies on bending radius of heterogeneous multicore fiber, in: *Optical Fiber Communication Conference*, Optical Society of America, 2013, pp. OTh3K–3.
- [15] Y. Amma, Y. Sasaki, K. Takenaga, S. Matsuo, J. Tu, K. Saitoh, M. Koshiba, T. Morioka, Y. Miyamoto, High-density multicore fiber with heterogeneous core arrangement, in: *Optical Fiber Communication Conference*, Optical Society of America, 2015, pp. Th4C–4.
- [16] J. Tu, K. Saitoh, M. Koshiba, K. Takenaga, S. Matsuo, Optimized design method for bend-insensitive heterogeneous trench-assisted multicore fiber with ultra-low crosstalk and high core density, *IEEE Journal of Lightwave Technology* 31 (2013) 2590–2598.
- [17] M. Koshiba, K. Saitoh, Y. Kokubun, Heterogeneous multi-core fibers: Proposal and design principle, *Electronic Express* 6 (2009) 98–103.
- [18] D. Kumar, R. Ranjan, Estimation of crosstalk in homogeneous multicore fiber for high core count under limited cladding diameter, in: *IEEE Information and Communication Technology*, 2017, pp. 1–4.
- [19] T. Mizuno, K. Shibahara, H. Ono, Y. Abe, Y. Miyamoto, F. Ye, T. Morioka, Y. Sasaki, Y. Amma, K. Takenaga, et al., 32-core dense SDM unidirectional transmission of PDM-16QAM signals over 1600 km using crosstalk-managed single-mode heterogeneous multicore transmission line, in: *IEEE Optical Fiber Communications Conference and Exhibition*, 2016, pp. 1–3.
- [20] M. Koshiba, K. Saitoh, K. Takenaga, S. Matsuo, Analytical expression of average power-coupling coefficients for estimating intercore crosstalk in multicore fibers, *IEEE Photonics Journal* 4 (2012) 1987–1995.
- [21] F. Ye, J. Tu, K. Saitoh, K. Takenaga, S. Matsuo, H. Takara, T. Morioka, Design of homogeneous trench-assisted multi-core fibers based on analytical model, *Journal of Lightwave Technology* 34 (2016) 4406–4416.
- [22] A. Filipenko, O. Sychova, Research of misalignments and cross-sectional structure influence on optical loss in photonic crystal fibers connections, in: *IEEE International Conference on Advanced Optoelectronics and Lasers*, 2013, pp. 85–87.
- [23] D. Marcuse, Loss analysis of single-mode fiber splices, *Bell System Technical Journal* 56 (1977) 703–718.
- [24] K. Watanabe, T. Saito, Compact fan-out for 19-core multicore fiber, with high manufacturability and good optical properties, in: *IEEE Optoelectronics and Communications Conference*, 2015, pp. 1–3.
- [25] J. Cui, S. Zhu, K. Feng, D. Hong, J. Li, J. Tan, Fan-out device for multicore fiber coupling application based on capillary bridge self-assembly fabrication method, *Optical Fiber Technology* 26 (2015) 234–242.
- [26] K.-P. Ho, J. M. Kahn, Mode-dependent loss and gain: statistics and effect on mode-division multiplexing, *Optics express* 19 (2011) 16612–16635.
- [27] A. Lobato, J. Rabe, F. Ferreira, M. Kuschnerov, B. Spinnler, B. Lankl, Near-ML detection for MDL-impaired few-mode fiber transmission, *Optics express* 23 (2015) 9589–9601.
- [28] K. Guan, P. J. Winzer, M. Shtaiif, BER performance of MDL-impaired MIMO-SDM systems with finite constellation inputs, *IEEE Photonics Technology Letters* 26 (2014) 1223–1226.
- [29] C. R. Schwarz, Statistics of range of a set of normally distributed numbers, *Journal of surveying engineering* 132 (2006) 155–159.
- [30] T. Ishigure, K. Ohdoko, Y. Ishiyama, Y. Koike, Mode-coupling control and new index profile of gi pof for restricted-launch condition in very-short-reach networks, *Journal of Lightwave Technology* 23 (2005) 4155–4168.
- [31] D. Polani, *Kullback-Leibler Divergence*, Springer New York, New York, NY, 2013, pp. 1087–1088.